Effects of atomic motion on the polarization properties of phase conjugation by two-photon-resonant degenerate four-wave mixing

Martti Kauranen and Robert W. Boyd
The Institute of Optics, University of Rochester, Rochester, New York 14627
(Received 10 December 1990)

We have studied the polarization properties of phase conjugation by degenerate four-wave mixing utilizing the $3S \rightarrow 4S$ two-photon-allowed transition of sodium. We have observed high-fidelity vector phase conjugation (simultaneous conjugation of the optical wave front and the state of polarization) at a reflectivity of $\sim 1\%$ for the case where the states of polarization of the two counterpropagating pump waves were circular and counterrotating. High-fidelity polarization conjugation with high reflectivity was obtained only when the forward pump wave was much stronger than the backward pump wave. To explain these results, it is necessary to include the effects of grating washout due to atomic motion in the theoretical analysis.

I. INTRODUCTION

It is well known that phase conjugation can be used for aberration correction of optical wave fronts when the incident field passes twice in opposite directions through the aberrating medium [1]. This wave-front-aberration correction property relies on the fact that the field amplitude of the conjugate field is the complex conjugate of that of the incident field. In an analogous manner, the state of polarization of an optical field can become distorted. To correct for polarization distortions, a phase-conjugate process should also have the property of polarization conjugation, where the polarization unit vector of the conjugate field is the complex conjugate of that of the incident field. A process that performs both wave-front conjugation and polarization conjugation can be thought of as an ideal phase-conjugate process and is often called vector phase conjugation (VPC).

Most theoretical studies of the polarization properties of phase conjugation have been performed in the limit of third-order theory [2-11]. In particular, Grynberg [2] and Ducloy and Bloch [3,4] have shown that degenerate four-wave mixing (DFWM) will lead to perfect VPC for arbitrary states of polarization of the two pump waves if the process is resonantly enhanced by a two-photon transition between two states of equal angular momenta J, with $J=0$ or $\frac{1}{2}$. This prediction has been tested experimentally by Malcuit, Gauthier, and Boyd [12] using the $3S \rightarrow 6S$ two-photon transition of sodium and linear and parallel pump wave polarizations. They observed high-fidelity VPC for pump intensities much lower than the two-photon saturation intensity, i.e., when the experiment can be adequately described by a third-order theory. In this experiment, a VPC reflectivity of the order of 10^{-5} was obtained. When the pump intensities were increased in order to increase the phase-conjugate reflectivity, the fidelity of the polarization conjugation process was found to be severely degraded. Polarization properties of phase conjugation have also been studied experimentally utilizing biexcitonic resonances [13], dyes held in a glass host [14], and stimulated Rayleigh-wing scattering [15].

In order to explain the experimental results of Ref. 12, we have recently developed a theory of DFWM resonantly enhanced by an atomic two-photon transition [16]. The theory treats the DFWM process for arbitrary states of polarization of the interacting fields, and includes the effects of saturation by the two counterpropagating pump fields. In the scalar limit, the theory reproduces the results of earlier work by Sargent, Ovadia, and Lu [17] and Fu and Sargent [18]. For the case of $S_0 \rightarrow S_0$ two-photon transition, which models the $3S \rightarrow 6S$ transition of sodium, the theory reveals two distinct mechanisms that can lead to the degradation of the fidelity of the VPC process when processes higher than third order occur. One of them is the transfer of population from the ground state to the two-photon-excited state. This process becomes important when the pump intensities are of the order of the two-photon saturation intensity. The other mechanism that can degrade the VPC process is the nonresonant Stark shift of the two-photon resonance frequency. This mechanism becomes important when the Stark shift is of the order of the population decay rate of the two-photon-excited state. For two-photon transitions with a large Stark shift, this effect may degrade the VPC process at pump intensities much lower than the two-photon saturation intensity. The theory was successful in explaining qualitatively the experimental results of Ref. 12.

The theory of Ref. 16 also shows that, when processes higher than third order become important, only the cases of linear and parallel and of circular and counterrotating pump wave polarizations can lead to high-fidelity VPC. Of these two cases, the case of circular and counterrotating pump wave polarizations is superior. In fact, the theory predicts that this case will always give rise to perfect VPC, even for arbitrarily high pump intensities, as long as the intensities of the two pump waves are equal.

In this paper, we present the results of an experimental study of the polarization properties of phase conjugation

by DFWM utilizing the $3S \rightarrow 4S$ two-photon transition of sodium. We chose to study the predictions of the theory described in Ref. 16 by using this transition since it has a smaller Stark shift and smaller saturation intensity than the $3S \rightarrow 6S$ transition. Consequently, we expect that we can obtain much higher VPC reflectivity at the $3S \rightarrow 4S$ transition than at the $3S \rightarrow 6S$ transition. We find experimentally that we can in fact achieve a much higher reflectivity ($\sim 1\%$) for this case. However, we find that high-fidelity VPC is obtained only when the forward pump wave is much more intense than the backward pump wave. These results are in agreement with the predictions of a modified theory that includes the effects of grating washout due to atomic motion.

II. REVIEW OF THEORY

In the theory of Ref. 16, the nonlinear medium was modeled as a collection of stationary atoms with a single ground state $|0\rangle$ connected through the intermediate states $|k\rangle$ to a single two-photon-excited state $|2\rangle$, as shown in Fig. 1. The atoms were assumed to interact with an electromagnetic field of the form

$$\mathbf{E}(\mathbf{r}) = \mathbf{E}_\omega(\mathbf{r})^{-i\omega t} + \mathbf{E}_\omega^*(\mathbf{r})e^{i\omega t} , \tag{1}$$

where 2ω is close to the two-photon transition frequency (i.e., $2\omega \approx \omega_{20}$, where $\hbar\omega_{20}$ is the energy difference between the excited and ground states). The density-matrix equations describing the nonlinear medium were solved in the steady state. These solutions were then used to obtain an expression for the nonlinear polarization driving the field at frequency ω.

The general expression for the nonlinear polarization at frequency ω given by Eq. (17) of Ref. 16 involves various summations over the intermediate states $|k\rangle$. These sums were evaluated for the special case of an $nS_0 \rightarrow n''S_0$ two-photon transition under the assumption that all interacting fields propagate almost parallel to the z axis. For this case, the only possible intermediate states $|k\rangle$ are the magnetic sublevels of the $n'P_1$ levels, as shown in Fig. 2, and the sums over the states $|k\rangle$ can be evaluated by expanding the polarization vectors in the circular basis with unit vectors $\hat{\mathbf{e}}_\pm = \mp(\hat{\mathbf{x}} \pm i\hat{\mathbf{y}})/\sqrt{2}$ and matrix elements $r_{ij}^{(\pm)} = \mp(x \pm iy)_{ij}/\sqrt{2}$ [19].

To study phase conjugation by DFWM, the total field at frequency ω was expressed as the sum

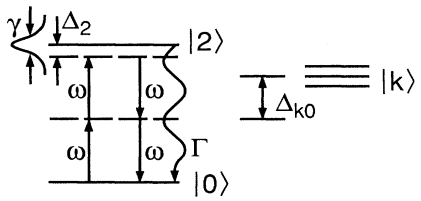

FIG. 1. Energy-level diagram showing the ground state $|0\rangle$ and the excited state $|2\rangle$, which are connected by two-photon transitions through the intermediate states $|k\rangle$. The two-photon transition has a linewidth γ and an effective population decay rate Γ from the excited state to the ground state.

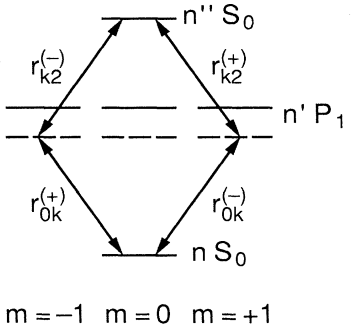

FIG. 2. Relevant states for the $nS_0 \rightarrow n''S_0$ two-photon excitation scheme. The matrix elements $r_{ij}^{(\pm)}$ operate between the transitions shown.

$$\mathbf{E}_\omega(\mathbf{r}) = \mathbf{E}_0(\mathbf{r}) + \mathbf{A}_p(\mathbf{r})e^{i\mathbf{k}_p\cdot\mathbf{r}} + \mathbf{A}_c(\mathbf{r})e^{-i\mathbf{k}_p\cdot\mathbf{r}} , \tag{2}$$

where $\mathbf{E}_0(\mathbf{r}) = A_f e^{i\mathbf{k}_0\cdot\mathbf{r}} + \mathbf{A}_b e^{-i\mathbf{k}_0\cdot\mathbf{r}}$ represents the field of the two counterpropagating pump waves, and $\mathbf{A}_p$ and $\mathbf{A}_c$ are the slowly varying amplitudes of the probe and conjugate fields, respectively. The probe and conjugate fields were assumed to be much weaker than the pump fields, and the expression for the nonlinear polarization was linearized with respect to the probe and conjugate fields.

To account for the polarization properties of phase conjugation, the amplitude of the probe field is represented as $\mathbf{A}_p = A_p\hat{\boldsymbol{\epsilon}}_p$, where $\hat{\boldsymbol{\epsilon}}_p$ is the complex polarization unit vector of the probe field. In the general case, the amplitude of the returning conjugate wave is represented as $\mathbf{A}_c = A_G\hat{\boldsymbol{\epsilon}}_G + A_B\hat{\boldsymbol{\epsilon}}_B$, where $\hat{\boldsymbol{\epsilon}}_G \equiv \hat{\boldsymbol{\epsilon}}_p^*$ is the polarization conjugate of the probe beam polarization (the "good" component or the polarization-conjugate component) and $\hat{\boldsymbol{\epsilon}}_B$ (the "bad" component) is the polarization unit vector orthogonal to $\hat{\boldsymbol{\epsilon}}_G$, i.e., $\hat{\boldsymbol{\epsilon}}_B \cdot \hat{\boldsymbol{\epsilon}}_G^* = 0$. For a high-fidelity VPC process, the amplitude of the good component should be much larger than the amplitude of the bad component, independent of the original state of polarization of the probe field.

In the limit of constant pump and probe field amplitudes, the theoretical results for the reflectivities associated with the good and bad polarization components of the conjugate field (R_G and R_B, respectively) are obtained from Eq. (28) of Ref. 16 by the following relations: $R_G = |\kappa_G|^2L^2$ and $R_B = |\kappa_B|^2L^2$, where L is the length of the nonlinear medium. The coupling strengths κ_G and κ_B can be expressed in terms of the linewidth γ of the two-photon transition, the effective population decay rate Γ from the two-photon-excited state $|2\rangle$ to the ground state $|0\rangle$, the detuning from the two-photon resonance $\Delta_2 = \omega_{20} - 2\omega$, the two-photon saturation intensity I_s, which can be expressed in units of electric field squared as

$$I_s = \frac{\hbar^2\sqrt{\gamma\Gamma}}{2e^2\left|\sum_k \frac{r_{2k}^{(+)}r_{k0}^{(-)}}{\omega_{k0}-\omega}\right|} , \tag{3}$$

and the Stark-shift parameter

$$\omega_S = -\frac{\sqrt{\gamma\Gamma}}{2} \frac{\sum_k \left[\frac{r_{2k}^{(+)} r_{k2}^{(-)}}{\omega_{2k}+\omega} + \frac{r_{2k}^{(+)} r_{k2}^{(-)}}{\omega_{2k}-\omega} + \frac{r_{0k}^{(+)} r_{k0}^{(-)}}{\omega_{k0}+\omega} + \frac{r_{0k}^{(+)} r_{k0}^{(-)}}{\omega_{k0}-\omega} \right]}{\left| \sum_k \frac{r_{2k}^{(+)} r_{k0}^{(-)}}{\omega_{k0}-\omega} \right|}, \tag{4}$$

which is defined in such a way that the Stark shift of the two-photon resonance frequency is $\Delta_S = \omega_S |\mathbf{E}_0|^2 / I_s$. Note that these definitions for the saturation intensity and the Stark-shift parameter are different from those of Ref. 16, which included only the contributions from the intermediate states closest to one-photon resonance. The expressions given by Eqs. (3) and (4) include contributions from all possible intermediate states [20]. This distinction is important in the case of the $3S \rightarrow 4S$ transition of sodium, where the dominant contribution to the Stark-shift parameter arises from the $4P$ state, which is not the state closest to one-photon resonance. Note also that the Stark shift Δ_S depends only on the atomic matrix elements and the total intensity, and is independent of the linewidth γ and the decay rate Γ of the transition.

III. EXPERIMENT

Our experimental setup is shown schematically in Fig. 3. The sodium vapor was contained in a heat-pipe oven with an interaction length of ~ 20 cm. The atomic number density was 10^{16}–10^{17} atoms/cm^3 and the helium buffer gas pressure was ~ 2 Torr. However, we take the actual number density of the vapor to be a free parameter which is used to fit the experimental results to the theoretical predictions. To excite the $3S \rightarrow 4S$ two-photon transition of sodium, an excimer-laser-pumped LDS-751 dye laser was operated at the wavelength of 777 nm with pulse energy of up to 3 mJ, pulse length of ~ 10 ns, and bandwidth of ~ 1.2 GHz. The output of the dye laser was weakly focused with a 2-m focal length lens giving a beam diameter of ~ 2 mm at the sodium cell. Optical path lengths for all interacting beams from the laser to the center of the sodium cell were equal within ~ 5 cm. The output of the dye laser was vertically polarized and the polarizations of the two pump beams were independently controlled by two Soleil-Babinet compensators (SBC). The intensity of the probe wave was always less than 1% of the intensities of the pump beams. The polarization of the probe wave was controlled by a quarter-wave plate (QWP). The extinction ratio of all polarizers was better than one part in ~ 40. The angle between the forward pump beam and the probe beam was held at $\sim 0.4°$ so that all beams overlapped throughout the entire sodium region.

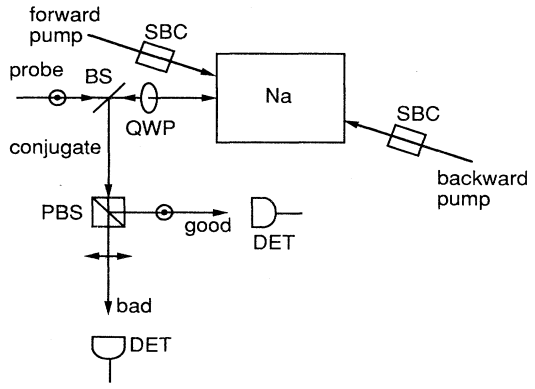

FIG. 3. The experimental setup shown schematically with the Soleil-Babinet compensators (SBC), the quarter-wave plate (QWP), the beam splitter (BS), the polarizing beam splitter (PBS), and the detectors (DET).

The quarter-wave plate acts as a known polarization aberrator for the probe wave. After reflecting from the sodium phase-conjugate mirror and passing again through the wave plate, the good polarization component of the conjugate field will become a vertical polarization component (i.e., the state of polarization of the probe wave before the wave plate) and the bad component will become a horizontal polarization component. The two polarization components of the conjugate beam can then be separated by using a polarizing beam splitter (PBS). By recording the intensities of the two components with two separate detectors (DET) we can quantify the fidelity of the VPC process.

The linewidth of the $3S \rightarrow 4S$ transition of sodium for our experimental conditions can be estimated from the measured low-intensity line shapes of the DFWM signal and was found to be $\gamma = 8 \times 10^9$ s^{-1}. We have found theoretically that the polarization properties of the VPC process become severely degraded when the pump intensity is so large that the Stark shift Δ_S becomes approximately equal to 2Γ. The Stark shift can be calculated from the known values of the atomic matrix elements [21] and the maximum pump intensity of approximately 3 MW/cm^2. The estimate for the population decay rate then becomes $\Gamma = 0.025\gamma$. This yields an estimate for the two-photon saturation intensity of approximately $I_s = 6$ MW/cm^2. However, to get the best agreement between the theory and experiment, we have taken the saturation intensity to have the slightly lower value of $I_s = 4$ MW/cm^2. The Stark-shift parameter can then be taken to have the value of $\omega_S = 0.12\gamma$.

In our first set of experiments, we confirmed the results of Ref. 12 for the case of linear and parallel pump wave polarizations. The probe wave was chosen to be circularly polarized because this polarization represents the worst-case situation for this choice of pump wave polarizations. In Fig. 4(a) we show the measured reflectivities

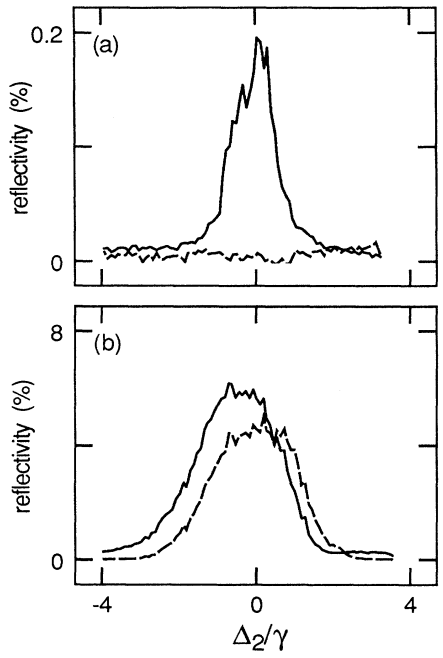

FIG. 4. The measured reflectivities associated with the good polarization component $\hat{\epsilon}_G = \hat{\epsilon}_p^*$ (solid line) and the bad polarization component $\hat{\epsilon}_B$ (dashed line) of the conjugate field as functions of the detuning Δ_2 from the two-photon resonance for the case of linear and parallel pump wave polarizations and a circularly polarized probe wave. (a) For a low pump wave intensity ($I_f = I_b = 0.016 I_s$), perfect VPC behavior is obtained. (b) For a high pump wave intensity ($I_f = I_b = 0.375 I_s$), the polarization character of the process is severely degraded.

associated with the good and bad polarization components of the conjugate wave as functions of the detuning Δ_2 from the two-photon resonance for the case where the forward and backward pump wave intensities, I_f and I_b, respectively, were equal to $I_f = I_b = 0.016 I_s$, where the two-photon saturation intensity is $I_s = 4$ MW/cm^2. We find that this case gives rise to high-fidelity VPC because the reflectivity for the good component is much higher than the reflectivity for the bad component. In Fig. 4(b) we show the line shapes of the two reflectivities for the case of high and equal pump wave intensities, $I_f = I_b = 0.375 I_s$. In this case, the reflectivities for the two polarization components of the conjugate field are comparable and the VPC character of the process is severely degraded. However, we were able to obtain a reflectivity of $\sim 0.2\%$ with good VPC fidelity utilizing the $3S \rightarrow 4S$ two-photon transition and linear and parallel pump wave polarizations. This value represents a factor of ~ 200 improvement compared to the results of Ref. 12. We believe that this improvement is due to the smaller Stark shift and the smaller saturation intensity of the $3S \rightarrow 4S$ transition.

In another set of experiments, we investigated the case of circular and counterrotating pump wave polarizations. This case is of interest because it has been predicted that this case should always give rise to perfect VPC when the intensities of the two pump waves are equal. For this choice of pump wave polarizations, a linearly polarized probe wave represents the worst-case situation. In Fig. 5(a) we show the reflectivities associated with the two polarization components of the conjugate field as functions of the detuning Δ_2 from the two-photon resonance for the case of $I_f = I_b = 0.375 I_s$. The corresponding theoretical line shapes based on the theory of Ref. 16 are shown in Fig. 5(b). In contrast to the theoretical prediction, the experimental plot shows that the reflectivity for the bad polarization component is comparable to the reflectivity for the good component. Hence the fidelity of VPC is severely degraded.

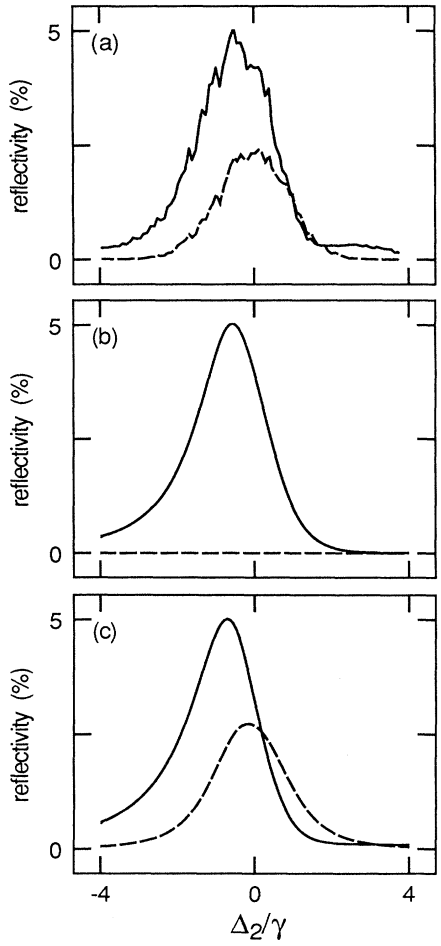

FIG. 5. Theoretical and experimental results for the reflectivities associated with the good polarization component $\hat{\epsilon}_G = \hat{\epsilon}_p^*$ (solid line) and the bad polarization component $\hat{\epsilon}_B$ (dashed line) of the conjugate field as functions of the detuning Δ_2 from the two-photon resonance for the case of circular and counterrotating pump wave polarizations and a linearly polarized probe wave. The pump wave intensities are $I_f = I_b = 0.375 I_s$. (a) The experimental results. (b) The theoretical predictions based on the theory of Ref. 16. (c) The theoretical predictions based on the modified theory which accounts for grating washout effects due to atomic motion.

To explain these new experimental results, we have modified the theory of Ref. 16 to include effects of grating washout due to atomic motion; the original theory assumed that the atoms are stationary. The details of this modification are explained in Sec. IV. The theoretical line shapes of the reflectivities associated with the two polarization components of the conjugate field calculated using the modified theory are shown in Fig. 5(c). We see that the agreement between the experimental and theoretical line shapes is now very good. The experimental results for the reflectivities were fitted to the theoretical predictions using the atomic number density as the fitting parameter so that the numerical values of the reflectivities for Figs. 5(a) and 5(c) agree.

The theory of Ref. 16 predicts that the VPC fidelity for the case of circular and counterrotating pump wave polarization depends sensitively on the imbalance between the forward and backward pump intensities. Therefore we have also investigated the effects of pump imbalance on the fidelity of VPC. In Fig. 6 we show the experimental and theoretical results for the reflectivities associated with the two polarization components of the conjugate field as functions of the detuning Δ_2 from the two-photon resonance for the case of $I_f+I_b=0.4I_s$, $I_f/I_b=\frac{1}{15}$. We see that lowering the forward pump intensity by a factor of 15 compared to the case of Fig. 5 has only a small effect on the phase-conjugate reflectivities or the fidelity of the VPC processes. In Fig. 7 we show the line shapes

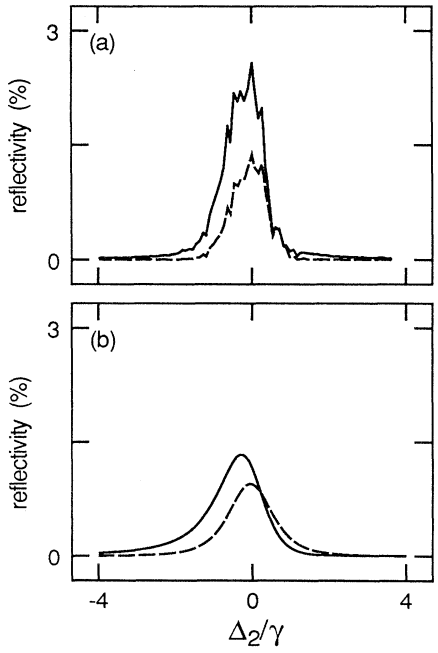

FIG. 6. Same as Fig. 5, but in the presence of pump wave intensity imbalance such that $I_f+I_b=0.4I_s$, $I_f/I_b=\frac{1}{15}$. (a) The experimental results. (b) The theoretical prediction based on the modified theory. The two reflectivities are lower than those of Fig. 5 by only a factor of 2, even though I_f has been lowered by a factor of 15.

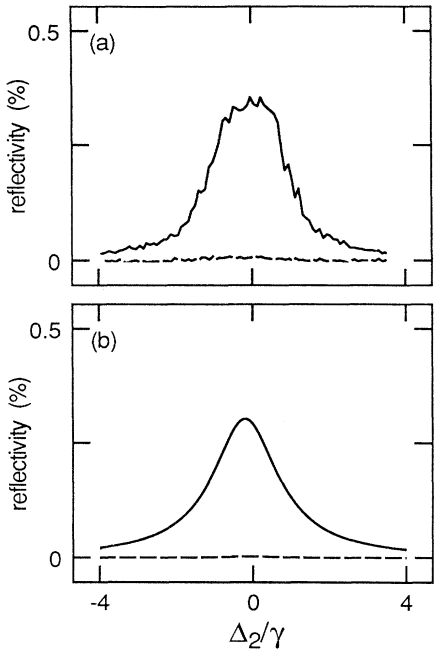

FIG. 7. Same as Figs. 5 and 6, but in the presence of pump wave intensity imbalance such that $I_f+I_b=0.4I_s$, $I_f/I_b=15$. (a) The experimental results. (b) The theoretical prediction based on the modified theory. The VPC fidelity is greatly improved compared to the cases of Figs. 5 and 6, but the phase-conjugate reflectivity is much lower for the current case.

of the two reflectivities for the case of $I_f+I_b=0.4I_s$, $I_f/I_b=15$. In this case, where the intensity of the backward pump wave has been lowered by a factor of 15 compared to the case of Fig. 5, the VPC fidelity is greatly improved compared to the cases of Figs. 5 and 6 but the reflectivity is lower by about a factor of 10. By carefully adjusting the imbalance between the forward and backward pump wave intensities while keeping the forward pump intensity at a value of $I_f=0.375I_s$, we have been able to obtain high-fidelity VPC at a reflectivity of $\sim 1\%$.

To illustrate further the effects of pump wave intensity imbalance on the fidelity of the VPC process, we have plotted in Fig. 8 the experimental and theoretical results for the reflectivities associated with the two polarization components of the conjugate wave as functions of pump intensity imbalance I_f/I_b and for the two-photon detuning Δ_2 that gives the maximum reflectivity for the good polarization component. We see that the fidelity of the VPC process can be improved only by making the forward pump intensity much stronger than the backward pump intensity, which leads to a large reduction in the phase-conjugate reflectivity.

In Figs. 5–8, we have investigated the fidelity of the VPC process only for a fixed state of polarization of the probe wave. For a true VPC process, the reflectivity associated with the good component must be much higher than the reflectivity associated with the bad component, and the reflectivities must be independent of the state of

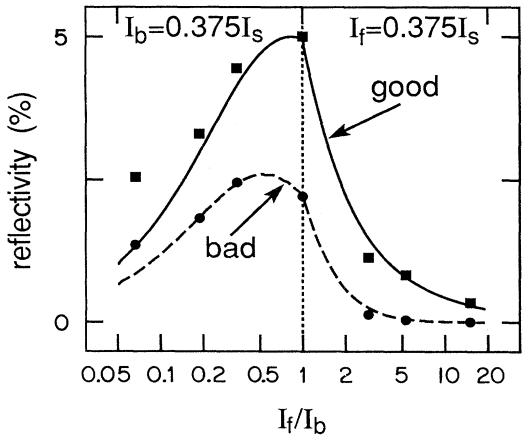

FIG. 8. Theoretical and experimental results for the reflectivities associated with the good and bad polarization components of the conjugate field as functions of the pump intensity imbalance I_f/I_b for the case of circular and counterrotating pump wave polarizations, a linearly polarized probe wave, and the detuning Δ_2 for which the reflectivity associated with the good component is maximum. High-fidelity VPC can only be obtained for the case where the forward pump wave is considerably stronger than the backward pump wave.

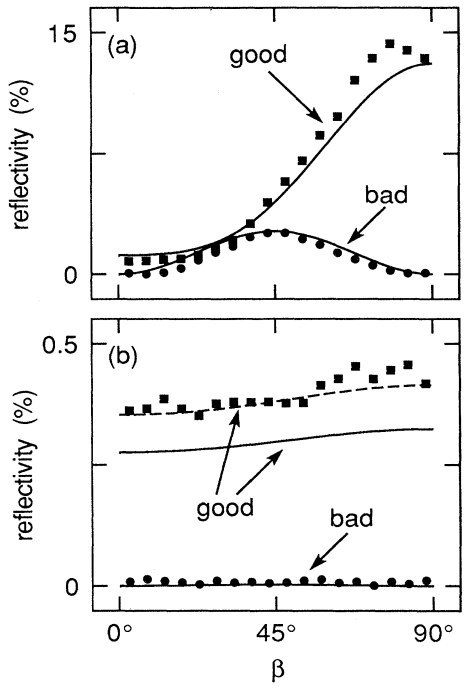

FIG. 9. Theoretical and experimental results for the reflectivities associated with the good and bad polarization components of the conjugate field as functions of the parameter β describing the state of polarization of the probe field [see Eq. (9)] for the case of circular and counterrotating pump wave polarizations and for the detuning $\Delta_2=-0.35\gamma$. (a) For high and equal pump wave intensities ($I_f=I_b=0.375I_s$), the results depend strongly on the state of polarization of the probe wave, and consequently the fidelity of VPC is poor. (b) The case of $I_f+I_b=0.4I_s$, $I_f/I_b=15$ gives rise to high-fidelity VPC, since the bad component vanishes and the good component is almost constant for any value of β. The dashed line shows the theoretical prediction for the case where the atomic number density is assumed to have a value such that theoretical and experimental results exactly agree for the value of β of 45°.

polarization of the probe wave. We have investigated this dependence by changing the angle of the wave plate so that the state of polarization of the incident probe field changes continuously from left-hand circular to linear to right-hand circular. This corresponds to varying the parameter β of Eq. (34) of Ref. 16 [which expresses the state of polarization of the probe wave in the circular basis as $\hat{\epsilon}_p=-(\cos\beta)\,\hat{e}_- -(\sin\beta)e^{i\eta}\,\hat{e}_+$] from 0° to 90°. In Fig. 9(a) we have plotted the experimental and theoretical results for the reflectivities associated with the two polarization components of the probe field as functions of the parameter β for the case where both pump intensities are equal, $I_f=I_b=0.375I_s$, and for the detuning $\Delta_2=-0.35\gamma$ from the two-photon resonance. We see that the reflectivities show strong variations as a function of parameter β. Consequently, this case does not give rise to high-fidelity VPC. In Fig. 9(b) we have repeated the plot of Fig. 9(a) for the case of Fig. 7 ($I_f+I_b=0.4I_s$, $I_f/I_b=15$). In this case, the reflectivity for the bad component is always much smaller than that for the good component. Moreover, the reflectivity for the good component is virtually constant for any value of β and consequently high-fidelity VPC is obtained. Note that, for this case, there is some discrepancy between the experimental and theoretical results for the magnitude of the reflectivity for the two polarization components of the conjugate field, although the general trend in both cases is the same. This discrepancy is due to the fact that we have chosen the value of our fitting parameter (the atomic number density) in such a way that the experimental and theoretical results exactly agree for the case of Fig. 5. The dashed line shows the theoretical prediction if the fitting parameter is chosen in such a way that the experimental and theoretical results exactly agree for the present case for $\beta=45°$.

These experimental results show that the polarization properties of phase conjugation by DFWM utilizing two-photon atomic resonances are strongly affected by grating washout effects resulting from atomic motion. The grating washout effects dramatically reduce the VPC reflectivity that can be obtained at two-photon transitions even when circular and counterrotating pump wave polarizations are used.

IV. INCLUSION OF GRATING WASHOUT EFFECTS IN THE THEORY

The nonlinear polarization of the atomic medium that represents the coupling from the probe field into the conjugate field can be expressed according to Eq. (22) of Ref. 16 as

$$\mathbf{P}_c(\mathbf{E}_p^*)=f_0(\mathbf{E}_0)(\mathbf{E}_0\cdot\mathbf{E}_0)\mathbf{E}_p^*+f_1(\mathbf{E}_0)(\mathbf{E}_0\cdot\mathbf{E}_p^*)\mathbf{E}_0 +f_2(\mathbf{E}_0)(\mathbf{E}_0^*\cdot\mathbf{E}_p^*)\mathbf{E}_0+f_3(\mathbf{E}_0)(\mathbf{E}_0\cdot\mathbf{E}_p^*)\mathbf{E}_0^* +f_4(\mathbf{E}_0)(\mathbf{E}_0^*\cdot\mathbf{E}_p^*)\mathbf{E}_0^* , \quad (5)$$

where the scalar line-shape functions $f_i(\mathbf{E}_0)$ depend on the atomic parameters and include saturation effects due to the pump fields. In Eq. (5) the total pump field is

$$\mathbf{E}_0(\mathbf{r})=\mathbf{A}_f e^{i\mathbf{k}_0\cdot\mathbf{r}}+\mathbf{A}_b e^{-i\mathbf{k}_0\cdot\mathbf{r}} , \quad (6)$$

and the probe field is

$$\mathbf{E}_p(\mathbf{r})=\mathbf{A}_p e^{i\mathbf{k}_p\cdot\mathbf{r}} . \quad (7)$$

We assume that the nonlinear medium is sufficiently thin that the amplitudes $\mathbf{A}_f$, $\mathbf{A}_b$, and $\mathbf{A}_p$ can be taken to be constant. We also assume that the wave vectors $\mathbf{k}_0$ and $\mathbf{k}_p$ are almost parallel to the z axis. Note that the polarization $\mathbf{P}_c$ of Eq. (5) is defined in terms of the probe field amplitude $\mathbf{E}_p$ whereas that defined by Eq. (22) of Ref. 16 is defined in terms of the spatially slowly-varying amplitude $\mathbf{A}_p$. Keeping the fast spatial variations in the current treatment is necessary for accounting for grating washout effects. The polarization properties of the interaction are determined by terms like $(\mathbf{E}_0\cdot\mathbf{E}_p^*)\mathbf{E}_0$ and $(\mathbf{E}_0^*\cdot\mathbf{E}_p^*)\mathbf{E}_0$ in Eq. (5). Note that the first term in Eq. (5) has the polarization vector $\hat{\boldsymbol{\epsilon}}_p^*$ and thus leads directly to VPC.

For the case of linear and parallel pump wave polarizations, the line-shape functions $f_i(\mathbf{E}_0)$ contain extremely complicated spatial variations. Hence it is very difficult to extract from Eq. (5) the gratings that persist after grating washout effects are accounted for. Fortunately, for the case of circular and counterrotating pump wave polarizations, the line-shape functions are spatially constant, and it is straightforward to account for the effects of grating washout. For simplicity, we will focus our attention on the case of circular and counterrotating pump wave polarizations in the following treatment.

In the case of circular and counterrotating pump wave polarizations, we express the total pump field as

$$\mathbf{E}_0=A_f e^{i\mathbf{k}_0\cdot\mathbf{r}}\hat{\mathbf{e}}_+ + A_b e^{-i\mathbf{k}_0\cdot\mathbf{r}}\hat{\mathbf{e}}_- . \quad (8)$$

We thus see that the product $\mathbf{E}_0\cdot\mathbf{E}_0=-2A_fA_b$ is spatially uniform. As mentioned above, for this choice of pump wave polarizations, the line-shape functions $f_i(\mathbf{E}_0)$ are also spatially uniform. Therefore the first term of Eq. (5), which always gives rise to perfect VPC, is not affected by grating washout effects. To account for grating washout effects in the remaining terms, we need to consider the field-dependent factors such as $(\mathbf{E}_0\cdot\mathbf{E}_p^*)\mathbf{E}_0$ and $(\mathbf{E}_0^*\cdot\mathbf{E}_p^*)\mathbf{E}_0$. Note that only the second term in Eq. (5) contains a factor that can be interpreted in the usual holographic picture of four-wave mixing in which an intensity pattern is recorded in the nonlinear medium and subsequently read out by another field. However, all of these terms in Eq. (5) contain spatial variations due to the spatial variations in the inversion between the two-photon-excited state $|2\rangle$ and the ground state $|0\rangle$ or the two-photon coherence between these states. More explicitly, it can be shown that the second and third terms correspond to gratings $\mathbf{E}_0\cdot\mathbf{E}_p^*$ and $\mathbf{E}_0^*\cdot\mathbf{E}_p^*$, respectively, which are recorded in the inversion, and which are read out with the field $\mathbf{E}_0$. The fourth and fifth terms correspond to similar gratings, which are recorded in the two-photon coherence, and which are read out with $\mathbf{E}_0^*$.

For the present choice of pump wave polarizations (circular and counterrotating), we find it convenient to express an arbitrary state of polarization of the probe field in the circular basis as [16]

$$\hat{\boldsymbol{\epsilon}}_p=-(\cos\beta)\,\hat{\mathbf{e}}_- -(\sin\beta)e^{i\eta}\,\hat{\mathbf{e}}_+ . \quad (9)$$

The factor $\mathbf{E}_0\cdot\mathbf{E}_p^*$, for example, then becomes

$$\mathbf{E}_0\cdot\mathbf{E}_p^*=(\hat{\mathbf{e}}_+\cdot\hat{\boldsymbol{\epsilon}}_p^*)A_f A_p^* e^{i(\mathbf{k}_0-\mathbf{k}_p)\cdot\mathbf{r}} +(\hat{\mathbf{e}}_-\cdot\hat{\boldsymbol{\epsilon}}_p^*)A_b A_p^* e^{-i(\mathbf{k}_0+\mathbf{k}_p)\cdot\mathbf{r}} . \quad (10)$$

The primary assumption of our new model is that the efficiency of a grating resulting from a physical process with a characteristic time constant τ will be decreased by the effects of atomic motion to a degree that depends on the fraction of the period l of the grating traveled by an average atom during the time τ. We require that the functional form for the efficiency possess the following properties: (1) it stays very close to unity for those cases where an average atom moves only over a small fraction of the grating period in time τ, and (2) it vanishes for those cases where an atom, on the average, travels at least half a period of the grating in time τ. These requirements are fulfilled by the following convenient choice for the amplitude efficiency:

$$S(\tau,l)=\begin{cases}\frac{1}{2}\left[1+\cos\left[2\pi\frac{v_{\mathrm{av}}\tau}{l}\right]\right], & v_{\mathrm{av}}\tau<l/2\\ 0, & v_{\mathrm{av}}\tau\geq l/2\end{cases} , \quad (11)$$

where v_{av} is the average thermal speed of an atom.

For our experimental conditions where the angle between the vectors $\mathbf{k}_0$ and $\mathbf{k}_p$ was $\sim 0.4°$, the first term of Eq. (10) represents a grating with a spatial period of approximately $l_1=2\pi/(k\tan 0.4°)=\lambda/\tan 0.4°\approx 110\ \mu$m (where $k=|\mathbf{k}_0|=|\mathbf{k}_p|$). The second term represents a grating with a period of approximately $l_2=2\pi/2k=\lambda/2\approx 0.39\ \mu$m. The average speed of a sodium atom in our experiment ($M=23$ a.u., $T=770$ K) was $v_{\mathrm{av}}=(2k_BT/M)^{1/2}\approx 750$ m/s. In the characteristic times $\tau_1=1/\Gamma\approx 5\times 10^{-9}$ s and $\tau_2=1/\gamma\approx 10^{-10}$ s, an average atom moves 75 nm and 3.8 μm, respectively. The effective contribution from Eq. (10) is then

$$\mathbf{E}_0\cdot\mathbf{E}_p^*=(\hat{\mathbf{e}}_+\cdot\hat{\boldsymbol{\epsilon}}_p^*)S(\tau,l_1)A_f A_p^* e^{i(\mathbf{k}_0-\mathbf{k}_p)\cdot\mathbf{r}} +(\hat{\mathbf{e}}_-\cdot\hat{\boldsymbol{\epsilon}}_p^*)S(\tau,l_2)A_b A_p^* e^{-i(\mathbf{k}_0+\mathbf{k}_p)\cdot\mathbf{r}} , \quad (12)$$

and the factor $(\mathbf{E}_0\cdot\mathbf{E}_p^*)\mathbf{E}_0$ resulting from the inversion becomes

$$(\mathbf{E}_0\cdot\mathbf{E}_p^*)\mathbf{E}_0=\hat{\mathbf{e}}_-(\hat{\mathbf{e}}_+\cdot\hat{\boldsymbol{\epsilon}}_p^*)S(\tau_1,l_1)A_f A_b A_p^* e^{-i\mathbf{k}_p\cdot\mathbf{r}} +\hat{\mathbf{e}}_+(\hat{\mathbf{e}}_-\cdot\hat{\boldsymbol{\epsilon}}_p^*)S(\tau_1,l_2)A_f A_b A_p^* e^{-i\mathbf{k}_p\cdot\mathbf{r}} , \quad (13)$$

where we have only kept the phase-matched contribution proportional to $e^{-i\mathbf{k}_p\cdot\mathbf{r}}$. By repeating a similar analysis of all factors like $(\mathbf{E}_0\cdot\mathbf{E}_p^*)\mathbf{E}_0$, it can be shown that the expressions for the coupling strengths κ_G and κ_B given by Eq. (28) of Ref. 16 remain valid, if the coefficients G_i and B_i are taken to be given by the expressions

$$
\begin{aligned}
G_1 &= -\frac{S(\tau_1,l_1)\sin^2\beta+S(\tau_1,l_2)\cos^2\beta}{I_f+I_b}A_f A_b \ , \\
G_2 &= \frac{I_b S(\tau_1,l_1)\sin^2\beta+I_f S(\tau_1,l_2)\cos^2\beta}{I_f+I_b} \ , \\
G_3 &= \frac{I_f S(\tau_2,l_1)\sin^2\beta+I_b S(\tau_2,l_2)\cos^2\beta}{I_f+I_b} \ , \\
G_4 &= -\frac{S(\tau_2,l_1)\sin^2\beta+S(\tau_2,l_2)\cos^2\beta}{I_f+I_b}A_f^* A_b^* \ ,
\end{aligned}
\tag{14}
$$

$$
\begin{aligned}
B_1 &= -\frac{[S(\tau_1,l_1)-S(\tau_1,l_2)]\sin\beta\cos\beta}{I_f+I_b}A_f A_b \ , \\
B_2 &= \frac{[S(\tau_1,l_1)I_b-S(\tau_1,l_2)I_f]\sin\beta\cos\beta}{I_f+I_b} \ , \\
B_3 &= \frac{[S(\tau_2,l_1)I_f-S(\tau_2,l_2)I_b]\sin\beta\cos\beta}{I_f+I_b} \ , \\
B_4 &= -\frac{[S(\tau_2,l_1)-S(\tau_2,l_2)]\sin\beta\cos\beta}{I_f+I_b}A_f^* A_b^* \ .
\end{aligned}
$$

For our experimental parameters, the efficiencies become

$$
\begin{aligned}
&S(\tau_1,l_1)=1, \quad S(\tau_1,l_2)=0 \ , \\
&S(\tau_2,l_1)=1, \quad S(\tau_2,l_2)=0.7 \ .
\end{aligned}
\tag{15}
$$

The theoretical predictions in Figs. 5(c)–9 were obtained using the theory of Ref. 16 with the coefficients G_i and B_i given by Eqs. (14) and (15) of the present paper. Equations (14) and (15) show that, due to the unequal values of $S(\tau,l_1)$ and $S(\tau,l_2)$, the coefficients B_i no longer vanish for equal pump wave intensities. The asymmetry between the forward and backward pump waves resulting from atomic motion therefore prevents the complete destructive interference occurring between the contributions in B_i arising from the backward and forward pump waves. Atomic motion thus leads to the degradation of VPC even in the case of circular and counterrotating pump wave polarizations when processes higher than third order become important.

V. CONCLUSIONS

We have investigated the polarization properties of phase conjugation by degenerate four-wave mixing at the two-photon-resonant $3S\rightarrow 4S$ transition of sodium. Using linear and parallel pump wave polarizations we have obtained a reflectivity of $\sim 0.2\%$ with good VPC fidelity. This value is a factor of ~ 200 higher than observed earlier under similar experimental conditions at the $3S\rightarrow 6S$ two-photon transition of sodium.

We have shown experimentally that the case of circular and counterrotating pump wave polarizations does not give rise to VPC for the case of equal forward and backward pump wave intensities if the total pump intensity is of the order of the two-photon saturation intensity. This result is in contrast with the predictions of a recent theoretical model that ignores the effects of atomic motion. We have been able to explain the experimental results by modifying the original theory to include grating washout effects due to atomic motion. Atomic motion breaks the symmetry between the forward and backward pump waves and thereby leads to the degradation of VPC fidelity of the process. High-fidelity VPC can be obtained by making the forward pump wave much stronger than the backward pump wave, but doing so leads to a significant reduction in the phase-conjugate reflectivity. This choice of pump intensity imbalance compensates for the unequal efficiencies of gratings formed by the forward and backward pump waves and allows an improved degree of destructive interference between the contributions arising from respective pump waves in the dominant contribution leading to the degradation of VPC fidelity under our experimental conditions. The highest reflectivity obtained with good VPC fidelity using circular and counterrotating pump wave polarizations was $\sim 1\%$.

ACKNOWLEDGMENTS

We gratefully acknowledge discussions of this work with M. S. Malcuit and D. J. Gauthier. We also acknowledge the help of R. E. Bridges at the initial stage of the experiments. This work was supported by the NSF Grant No. ECS-8802761 and by the U.S. Army Research office through the University Research Initiative.

[1] *Optical Phase Conjugation,* edited by R. A. Fisher (Academic, New York, 1983).
[2] G. Grynberg, Opt. Commun. **48**, 432 (1984).
[3] M. Ducloy and D. Bloch, Phys. Rev. A **30**, 3107 (1984).
[4] M. Ducloy, R. K. Raj, and D. Bloch, Opt. Lett. **7**, 60 (1982).
[5] S. Saikan and M. Kiguchi, Opt. Lett. **7**, 555 (1982).
[6] S. Saikan, J. Opt. Soc. Am. **72**, 514 (1982).
[7] G. Martin, L. L. Lam, and R. W. Hellwarth, Opt. Lett. **5**, 185 (1980).
[8] V. N. Blaschuk, B. Ya. Zel'dovich, A. V. Mamaev, N. F. Pilipetsky, and V. V. Shkunov, Kvant. Elektron. (Moscow) **7**, 627 (1980) [Sov. J. Quantum Electron. **10**, 356 (1980)].
[9] T. Wilson, D. K. Saldin, and L. Solymar, Opt. Commun. **39**, 11 (1981).
[10] T. Wilson, D. K. Saldin, and L. Solymar, Opt. Acta **29**, 1041 (1982).
[11] P. Yeh, Opt. Commun. **51**, 195 (1984).

[12] M. S. Malcuit, D. J. Gauthier, and R. W. Boyd, Opt. Lett. **13**, 663 (1988).
[13] L. L. Chase, M. L. Claude, D. Hulin, and A. Mysyrowicz, Phys. Rev. A **28**, 3696 (1983).
[14] W. R. Tompkin, M. S. Malcuit, and R. W. Boyd, J. Opt. Soc. Am. B **6**, 757 (1989).
[15] E. J. Miller and R. W. Boyd, Opt. Lett. **15**, 1188 (1990).
[16] M. Kauranen, D. J. Gauthier, M. S. Malcuit, and R. W. Boyd, Phys. Rev. A **40**, 1908 (1989).
[17] M. Sargent III, S. Ovadia, and M. H. Lu, Phys. Rev. A **32**, 1596 (1985).
[18] T. Fu and M. Sargent III, Opt. Lett. **5**, 433 (1980).
[19] R. D. Cowan, *The Theory of Atomic Structure and Spectra* (University of California Press, Berkeley, 1981).
[20] L. Allen and C. R. Stroud, Jr., Phys. Rep. **91**, 1 (1982).
[21] R. B. Miles and S. E. Harris, IEEE J. Quantum Electron. **QE-9**, 470 (1973).